JOURNAL OF SOLID STATE CHEMISTRY **92,** 578–590 (1991)

Structures of Stoichiometric and Nonstoichiometric NH_4^+ β-Alumina Compounds and Their Thermal Properties

N. IYI, Y. YAJIMA, AND S. KIMURA

National Institute for Research in Inorganic Materials, Namiki 1-1, Tsukuba-shi, Ibaraki 305 Japan

Received August 6, 1990; in revised form January 28, 1991

The crystal structures of nonstoichiometric and stoichiometric NH_4^+ β-alumina compounds were refined by the single crystal X-ray diffraction method. They were synthesized by NH_4^+ ion exchange (200–210°C) from K β-aluminas ($K_{1+x}Al_{11}O_{17+x/2}$) of different nonstoichiometry ($x = 0.2$ and $x = 0.5$). The nonstoichiometric NH_4^+ β-alumina having a composition of $(NH_4)_{1.2}Al_{11}O_{17.1}$ was derived from a large single crystal of $K_{1.2}$ β-alumina ($x = 0.2$). The stoichiometric NH_4^+ β-alumina $(NH_4)_{1.0}Al_{11}O_{17.0}$ was derived from a very thin crystal of extremely nonstoichiometric $K_{1.5}$ β-alumina ($x = 0.5$). It contained only a stoichiometric amount of NH_4^+ ions and no interstitial Al and O ions were detected by the X-ray method. Though the cause of the difference in the exchange reaction is not pinpointed yet, it is clear that excess cations could be eliminated during the NH_4^+ ion-exchange under certain conditions in the β-alumina system. The thermal decomposition of these NH_4^+ β-aluminas were also discussed on the basis of TGA/DTA data and the lattice parameters.

Introduction

A wide variety of β-alumina compounds having protonic species have been reported (*1–5*). Among them, ammonium (NH_4^+) β-alumina (*6–8*) is one of the most interesting material from the viewpoint of structure as well as ionic conduction mechanism. This compound was first synthesized by Yao and Kummer (*2*) using molten NH_4NO_3 as the ion-exchange medium. In early 1980s, studies on the structure, thermal properties, conductivity, and other properties were published extensively (*6–11*).

NH_4^+ β-alumina has been produced by NH_4^+ ion-exchange reaction of Na^+ or K^+ β-alumina in molten NH_4NO_3 bath at about 200–210°C. The resulting NH_4^+ β-alumina is known to have a composition of $(NH_4)_{1+x}Al_{11}O_{17+x/2}$ ($x \approx 0.3$). Contrary to NH_4^+ β″-alumina (*12–14*), water and/or hydronium ions have not been detected by IR study (*4, 15*). The crystal structure analysis was accomplished by Colomban *et al.* (*6*) and Newsam *et al.* (*8*). Essentially, their results agree with each other. Excess NH_4^+ ions were found in the conduction plane and the Frenkel defect of the Al^{3+} ion and interstitial O^{2-} compensating for excess cation charge were discovered. In short, their results were: (i) NH_4^+ β-alumina contained neither water nor hydronium ions in its structure. (ii) The nonstoichiometry didn't change during NH_4^+ ion exchange and excess NH_4^+ ions remained in the structure. The thermal properties were also investigated in detail (*4, 6–8*) in connection with its potential use for battery fuel.

Recently, the NH_4^+ ion exchange reaction of potassium β-gallate, which has a β-alu-

0022-4596/91 $3.00

mina structure with the chemical formula $K_{1.25}Ga_{11.0}O_{17.125}$, was studied by Ikawa *et al.* (*16, 17*) and they reported that β-gallate lost excess NH_4^+ ions together with interstitial oxygen ions during NH_4^+ ion-exchange reaction, giving stoichiometric NH_4^+ β-gallate, $(NH_4)_{1.0}Ga_{11.0}O_{17.0}$. They also suggested a similar reaction would occur in a β-alumina system, and threw doubt on the composition of the resulting NH_4^+ β-alumina so far reported.

Thus, the problems of structure, composition of NH_4^+ β-alumina, and NH_4^+ ion-exchange reaction are not settled yet. To elucidate the NH_4^+ ion-exchange reaction of β-alumina, it was examined whether the (i) size of the crystal, (ii) amount of excess cation in the starting β-alumina, (iii) cation species of the starting β-alumina *etc.* influence the resulting composition of NH_4^+ β-alumina. In the course of the study we could obtain stoichiometric as well as nonstoichiometric NH_4^+ β-alumina. So far, several stoichiometric β-alumina compounds have been produced and analyzed (*6, 18*); however, no data have been published on the structure parameters of stoichiometric NH_4^+ β-alumina.

In the present paper the crystal structure of stoichiometric NH_4^+ β-alumina, as well as that of nonstoichiometric NH_4^+ β-alumina, is described, and their thermal behavior is discussed on the basis of the TGA/DTA and crystallographic data.

Experimental

1. Preparation

Two kinds of NH_4^+ β-alumina compounds were prepared by NH_4^+ ion exchange from K^+ β-alumina having different amounts of excess cations. They are designated as NH4-K and NH4-B in the present paper.

NH4-K was obtained by ion exchange from $K_{1.2}$ β-alumina which was derived from $Na_{1.2}$ β-alumina. $Na_{1.2}$ β-alumina (Toshiba Monoflux) crystals were confirmed to have a composition of $Na_{1.20}Al_{11.0}O_{17.1}$ by chemical analysis. This means 20% excess Na^+ over stoichiometry. $Na_{1.2}$ β-alumina single crystals used for ion-exchange were sliced into bars with 0.5 mm thickness in the *c*-plane. Conversion of $Na_{1.2}$ β-alumina into $K_{1.2}$ β-alumina was conducted by conventional K^+ ion exchange in molten KNO_3 at 380°C for 3 days. Sections of exchanged bars were checked by line scanning using EPMA (electron probe microanalyzer), and no remaining Na^+ ion was detected. The resulting crystals were wrapped in a Pt mesh bag, and NH_4^+ ions were substituted for K^+ by ion exchange in molten NH_4NO_3 at 200–210°C for 3 weeks. A polished section perpendicular to the *c*-direction showed no remaining K^+ ion by EPMA. The exchange scheme was

$$Na_{1.2}Al_{11.0}O_{17.1} \rightarrow K_{1.2}Al_{11.0}O_{17.1} \rightarrow \text{NH4-K}.$$

The starting material of NH4-B was Ba β-alumina ($Ba_{0.75}Al_{11.0}O_{17.25}$) which was grown by the floating zone (FZ) method (*19*). At first, Ba β-alumina was converted to K β-alumina, and then into NH_4^+ β-alumina by ion exchange. As the NH_4^+ ion exchange was very sluggish, the starting Ba β-alumina boules were cut and polished to thin plates with 100 μm thickness in the *c*-plane due to an extremely low exchange rate. Ba β-alumina was ion-exchanged into $K_{1.5}$ β-alumina in molten K_2CO_3 at 1000°C (*20, 21*). $K_{1.5}$ β-alumina was further converted to NH_4^+ β-alumina by an NH_4^+ ion exchange reaction at 200–210°C for a duration of more than 3 weeks. The obtained crystals still retained transparency. The ion exchange sequence was

$$Ba_{0.75}Al_{11}O_{17.25} \rightarrow K_{1.5}Al_{11}O_{17.25} \rightarrow \text{NH4-B}.$$

2. Characterization

The progress of the exchange was monitored by EPMA (JEOL, Shimadzu) operated at 15 kV. This method was also used for determination of the ion-exchange condition. Each time after ion exchange, the composition within the crystal was checked by the line scanning.

The NH_3 content was determined by the Kjeldahl method. After pulverized in an agate mortar, the specimen was dried at 100°C for 2 hr to eliminate adsorbed water, and then it was digested in concentrated H_2SO_4 solution at 160°C for 1 night under pressure, followed by steam distillation and titration. The recovery of the NH_3 after this treatment was estimated to be 99.5% on the basis of the standard material, $(NH_4)_2SO_4$. K^+, Na^+ ions were determined by atomic absorption analysis. The ingition loss was measured by heating the pulverized samples at 1100°C for 0.5 hr. This weight loss reflects the conversion of NH_4^+ β-alumina into α-alumina. Thermogravimetric (TGA) and differential thermal analyses (DTA) were carried out for NH4-K and NH4-B up to 1100°C on a TG-DTA apparatus (TAS-200, Rigaku Denki Co.). The heating rate was 5°C/min. TGA/DTA was carried out in flowing dry nitrogen as well as atmospheric air.

Refinements of the crystal structure were carried out for these NH_4^+ β-alumina compounds, NH4-K and NH4-B. Specimens were cut into rectangle crystals, among which some specimens having good shape were selected and the crystallinity was checked by the X-ray precession photographs. Selected crystals had a dimension of $105 \times 150 \times 80$ μm for NH4-K and $85 \times 120 \times 80$ μm for NH4-B. The X-ray photos (the Precession and Weisenberg methods) and electron diffraction (Hitachi H-500 operated at 100 kV) revealed that the structure belonged to the hexagonal space group $P6_3/mmc$ and showed no sign of superstructure. Using rectangular crystals, intensity data were collected on an automatic four-circle diffractometer (AFC-3, Rigaku Denki Co.) using graphite-monochromatized Mo$K\alpha$ radiation (λ = 0.71068 Å). The ω-2θ scanning was used for intensity data collections up to 2θ = 120°. The final set of nonzero independent reflections below 2θ = 120° was corrected for Lorenz polarization and absorption effects. The lattice parameters were determined on the basis of 2θ-data (20–25 reflections within 2θ = 50–90°, Mo$K\alpha 1$ radiation, λ = 0.70926 Å) collected on the four-circle diffractometer. An anisotropic absorption correction due to crystal shape was applied. Absorption correction was based on the algorithm of Busing and Levy (*22*). The neutral scattering factors were taken from Ref. (*23*). The full matrix least-squares program was a modified version of RSFLS-4 (*24*) and Fourier syntheses were done by using RSSFR-5 (*25*). Secondary extinction corrections were based on the algorithm of Becker and Coppens (*26*). The nomenclature of the sites in the mirror plane was taken after Peters *et al.* (*27*). The numbering of atoms was after Ref. (*28*).

High temperature X-ray powder diffraction was carried out on freshly ground NH4-K by using a diffractometer (RINT 1000, Rigaku). 2θ-Data within 2θ = 30–50° (Cu$K\alpha$ radiation, λ = 1.5418 Å) were collected at temperatures from 200 to 600°C at 50°C intervals and from 600 to 1100°C at 100°C intervals. The heating rate between the steps was 20°C/min. The scanning speed was 2°/min. The lattice parameters were calculated using the least-squares method.

Refinement

1. NH4-K

A set of 956 nonzero independent reflections was used for refinement. As the starting parameters, those of NH_4^+ β-alumina (6) were used assuming stoichiometric composition with no defects. Difference Fourier synthesis at this stage showed positive electron density at the *mO* site in the mirror plane, so N atoms were included in the refinement as N(2). Secondary extinction correction (Lorenzian, Type II) was also included in the next refinement leading to *R*

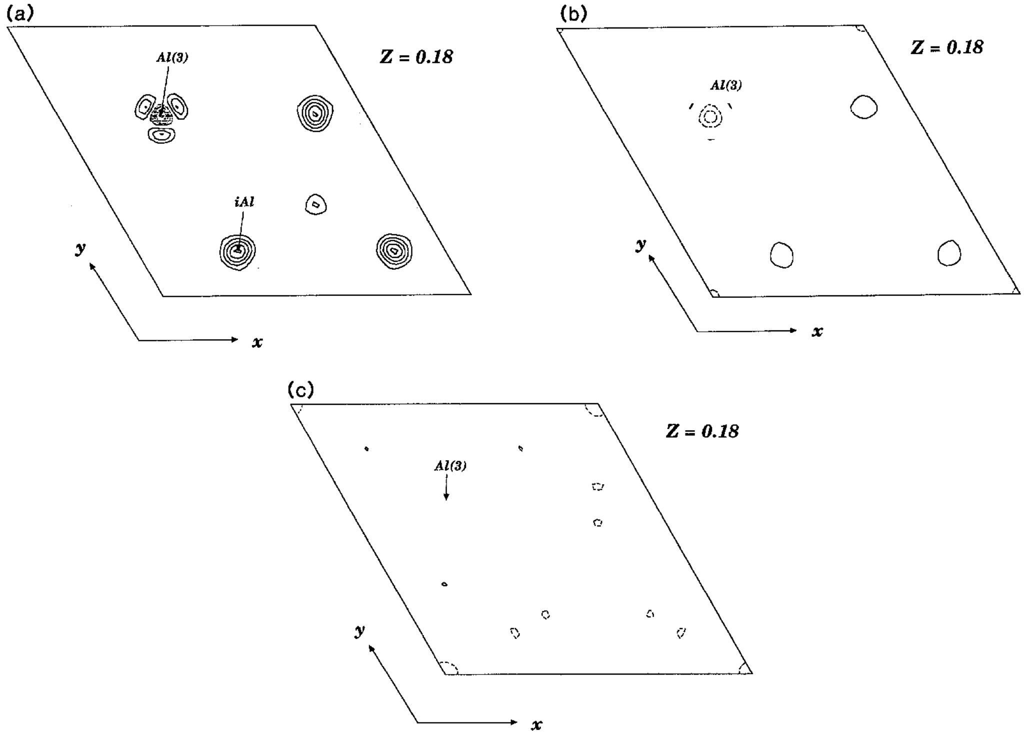

FIG. 1. Difference Fourier sections showing the electron density at $z = 0.18$ for (a) NH4-K ($R = 0.050$), (b) NH4-K heat treated at 370°C ($R = 0.037$), and (c) NH4-B ($R = 0.038$). Contour lines are drawn with the interval of 0.4 $eÅ^{-3}$. Dashed contour lines indicate negative electron density. Zero contours are omitted. The positions of Al(3) and *i*Al are indicated.

$= \Sigma\, ||F_o| - |F_c||/\Sigma\, |F_o| = 0.050$ ($wR = (\Sigma\, w(|F_o| - |F_c|)^2/\Sigma\, |F_o|^2)^{1/2} = 0.054$, $w = 1/\sigma F^2$, $S = [\Sigma\, w(|F_o| - |F_c|)^2/(m - n)]^{1/2} = 3.28$). (Secondary extinction correction without including N(2) led to $R = 0.055$. The difference Fourier map at $z = 0.25$ is shown in Fig. 2a.) Difference Fourier synthesis at this stage still indicated residual positive electron density at the 12*k* (0.83, 0.66, 0.18) (Fig. 1a), and 6*h* (0.86, 0.72, 0.25) sites, so interstitial ions were included in the next refinement as Al(5) and O(6). Final isotropic refinement yielded $R = 0.044$ ($wR = 0.049$, $w = 1/\sigma F^2$, $S = 2.95$). Anisotropic refinement was performed with the isotropic temperature factors of Al(5) and O(6) being fixed. The final anisotropic refinement gave a final *R*-value of 0.034 ($wR = 0.042$, $w = 1/\sigma F^2$, $S = 2.54$). The *g*-value was $1.76(5) \times 10^4$. The difference Fourier synthesis at the final stage showed random peaks and depressions in the range of -0.9 (at (0,0,0.10)) to $+0.7$ $eÅ^{-3}$ (at (0.4,0.15,0.09)).

The previous two works (*6, 8*) are consistent; however, there is a discrepancy in the excess N site. Colomban *et al.* (*6*) reported the N atom at the *aBR* site $(0,0,\frac{1}{4})$; Newsam *et al.* (*8*) did not observe any electron density at the *aBR* site. No extra electron density was observed in the Fourier sections in the course of the refinement, so we concluded that there were no NH_4^+ ions at the *aBR* site. Our results are in good agreement with the latter work. The crystallographic data are shown in Table I. The final parameters are given in Table II; the bond lengths

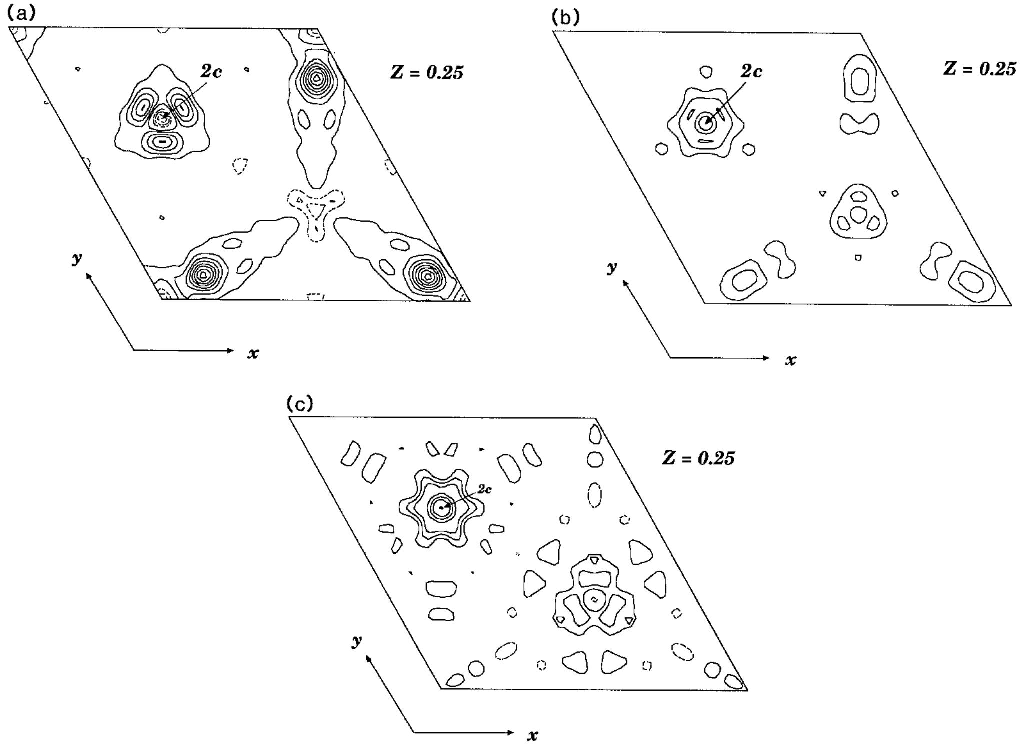

FIG. 2. Difference Fourier sections showing the electron density in the mirror plane at $z = 0.25$ for (a) NH4-K ($R = 0.055$), (b) NH4-K heat treated at 370°C ($R = 0.037$), and (c) NH4-B ($R = 0.038$). Contour lines are drawn with the interval of 0.4 eÅ^{-3}. Dashed contour lines indicate negative electron density. Zero contours are omitted.

and angles were presented in Tables IV and V, respectively.

To check the effects of the cation species of the starting material, the same characterization (chemical analysis, thermal behavior, structure refinement) was conducted on the NH_4^+ β-alumina ion exchanged directly from $Na_{1.2}$ β-alumina; the results showed no significant difference from those of NH4-K.

TABLE I

CRYSTALLOGRAPHIC DATA

	NH4-K	NH4-B
Formula	$(NH_4)_{1.2}Al_{11.0}O_{17.1}$	$(NH_4)_{1.0}Al_{11.0}O_{17.0}$
Symmetry	Hexagonal	Hexagonal
Space group	*P63/mmc*	*P63/mmc*
	$a = 5.5980(2)$ Å	5.5983(2) Å
	$c = 22.876(1)$ Å	22.843(1) Å
	$V = 620.83(5)$ Å^3	620.02(5) Å^3
	$Z = 2$	2
	Dcalc =3.17 g/cm^3	3.14 g/cm^3

2. *NH4-B*

A set of 659 nonzero independent reflections was used for refinement. As the starting parameters, those of NH_4^+ β-alumina (*6*) were used assuming stoichiometric composition with no defects. Isotropic refinement converged quickly to give an R-value of 0.038 ($wR = 0.048$, $w = 1/\sigma F^2$, $S = 3.72$). Difference Fourier syntheses at this stage showed no significant positive electron density. For the comparison with NH4-K, the difference Fourier map of the $z = 0.18$ layer

TABLE II

THE POSITIONAL AND THERMAL PARAMETERS OF NH4-K[a]

Position		Number per unit cell	x	z	β_{11}x10^4	β_{22}x10^4	β_{33}x10^5	β_{23}x10^5	B
N(1)	2d	1.74(9)	2/3	1/4	188(21)	β_{11}	33(8)	0	
N(2)	6h	0.87(11)	0.909(3)	1/4					1.2(4)
Al(1)	12k	11.49(9)	0.8322(1)	0.10450(4)	40(2)	33(2)	20(1)	-1(4)	
Al(2)	4f	4	1/3	0.02454(6)	28(2)	β_{11}	16(2)	0	
Al(3)	4f	4	1/3	0.17448(7)	59(2)	β_{11}	13(2)	0	
Al(4)	2a	2	0	0	36(3)	β_{11}	12(2)	0	
Al(5)	12k	0.44(4)	0.839(3)	0.1757(8)					0.19(26)
O(1)	12k	12	0.1570(2)	0.04928(7)	54(3)	33(4)	20(2)	-5(6)	
O(2)	12k	12	0.5019(3)	0.14427(7)	41(3)	44(4)	35(2)	8(7)	
O(3)	4f	4	2/3	0.0547(2)	47(4)	β_{11}	19(3)	0	
O(4)	4e	4	0	0.1400(1)	38(4)	β_{11}	20(3)	0	
O(5)	6h	2	0.326(4)	1/4	139(17)	357(112)	17(5)	0	
O(6)	6h	0.18(7)	0.854(7)	1/4					0.23(71)

[a] The thermal parameters are of the form: $\exp[-(h^2\beta_{11} + k^2\beta_{22} + l^2\beta_{33} + 2hk\beta_{12} + 2hl\beta_{13} + 2kl\beta_{23})]$. $\beta_{12} = \beta_{22}/2$; $\beta_{13} = \beta_{23}/2$. $y = 2x$.

is presented in Fig. 1c. Contrary to the Fourier map of NH4-K, it clearly shows no residual electron density at the interstitial Al^{3+} site. So interstitial ions were not included in the next anisotropic refinement. The anisotropic refinement yielded a R-value of 0.031 ($wR = 0.045$, $w = 1/\sigma F^2$, $S = 3.45$). The difference Fourier maps at this stage are shown in Fig. 3. Figure 3b shows residual peaks ($+0.8$ eÅ^{-3}) at the 12j site around the BR (2d) site, which corresponds to the position of H in NH_4^+ revealed by

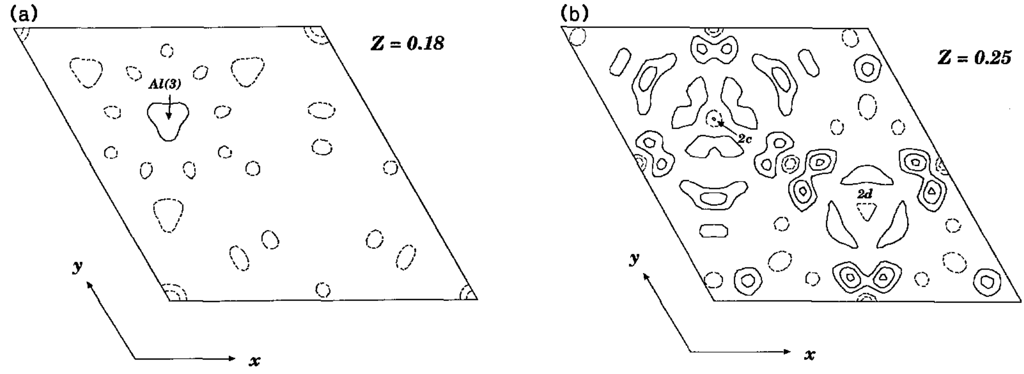

FIG. 3. Difference Fourier sections showing the electron density at $z = 0.18$ and 0.25 for NH4-B at $R = 0.030$. Contour lines are drawn with the interval of 0.25 eÅ^{-3}. Dashed contour lines indicate negative electron density. Zero contours are omitted.

TABLE III

THE POSITIONAL AND THERMAL PARAMETERS OF $(NH_4^+)_{1.0}$ β-ALUMINA[a]

Position		Number per unit cell	x		z	$\beta_{11}x10^{4}$	$\beta_{22}x10^{4}$	$\beta_{33}x10^{5}$	$\beta_{23}x10^{5}$	B
N	2d	2.01(4)	2/3		1/4	182(16)	β_{11}	35(7)	0	
Al(1)	12k	12	0.83254(8)		0.10538(2)	32(2)	29(2)	20(1)	3(4)	
Al(2)	4f	4	1/3		0.02487(4)	28(2)	β_{11}	12(1)	0	
Al(3)	4f	4	1/3		0.17487(5)	33(2)	β_{11}	13(1)	0	
Al(4)	2a	2	0		0	31(3)	β_{11}	13(2)	0	
O(1)	12k	12	0.1569(2)		0.04919(5)	41(3)	35(5)	15(1)	-2(7)	
O(2)	12k	12	0.5013(2)		0.14384(5)	33(3)	39(5)	22(1)	19(8)	
O(3)	4f	4	2/3		0.05478(9)	42(5)	β_{11}	16(3)	0	
O(4)	4e	4	0		0.1397(1)	32(5)	β_{11}	23(3)	0	
O(5)	2c	2	1/3		1/4	134(10)	β_{11}	8(4)	0	
			x	y	z					
H	12j	4.02^{c}	0.6^{b}	0.178(20)	1/4					1.0^{b}

[a] The thermal parameters are of the form: $\exp[-(h^2\beta_{11} + k^2\beta_{22} + l^2\beta_{33} + 2hk\beta_{12} + 2hl\beta_{13} + 2kl\beta_{23})]$. $\beta_{12} = \beta_{22}/2$; $\beta_{13} = \beta_{23}/2$. $y = 2x$ (except for H).

[b] Fixed.

[c] Constrained; $n(H) = 2.0 \times n(N)$; n, occupation number.

Newsam *et al.* (*8*). In the final refinement, H was introduced with the occupancy of N being varied. Here, the occupancy of H was constrained to twice of that of N, and the x-coordinate of H was also fixed. A secondary extinction correction was also introduced as the intense reflections $|F_o|$ were systematically smaller than $|F_c|$. The final anisotropic refinement gave a R-value of 0.029 (wR = 0.031, $W = 1/\sigma F^2$, S = 2.38). The g-value was $1.18(9) \times 10^3$. Final difference maps showed random peaks and depressions within the range −0.9 (at (0,0,0.1)) to +1.2 $e\text{Å}^{-3}$ (at (0,0,0)). The occupancy of N and lack of interstitials clearly indicate that NH4-B has stoichiometric composition. The crystallographic data are shown in Table I. The final parameters are given in Table III; the interatomic distances and bond angles are presented in Tables IV and V, respectively.

Results and Discussion

1. *Diffusion*

Figure 4a depicts the compositional profile of NH4-K during the ion-exchange process. It shows a typical diffusion profile. In the case of NH4-B, however, the progress of the NH_4^+ ion exchange is indicated by an exchange front visualized by the difference of the refractive index between the exchanged and the unexchanged layer. It caused a "photo frame" appearance in the basal plane. A similar phenomenon was already observed in the system of silver-ammonium β-alumina (*29*). The profile of the K-content across the crystal is shown in Fig.

TABLE IV

INTERATOMIC DISTANCES

	Number of bonds	Distance (Å)	
		NH4-K	NH4-B
	Octahedral coordination		
Al(1)- O(1)	2	2.021(2)	2.033(3)
- O(2)	2	1.842(2)	1.830(2)
- O(3)	1	1.968(3)	1.981(2)
- O(4)	1	1.818(2)	1.803(2)
Al(4)- O(1)	6	1.894(2)	1.891(2)
	Tetrahedral coordination		
Al(2)- O(1)	3	1.801(2)	1.799(2)
- O(3)	1	1.813(5)	1.819(3)
Al(3)- O(2)	3	1.775(3)	1.777(2)
- O(5)	1	1.729(3)	1.716(2)
Al(5)- O(2)	2	1.79(4)	
- O(4)	1	1.76(3)	
- O(6)	1	1.71(2)	
	Polyhedron 9-coordinated		
N(1) - O(2)	6	2.899(2)	2.907(2)
- O(5)	3	3.25(4) (averaged)	3.2322(1)
	Polyhedron 8-coordinated		
N(2) - O(2)	4	3.19(2)	
- O(4)	2	2.67(1)	
- O(5)	2	2.89(5) (averaged)	

TABLE V

BOND ANGLES

	Bond Angles (°)	
	NH4-K	NH4-B
	Octahedral coordination	
O(1)-Al(1)-O(1)'	81.45(11)	80.83(10)
O(1)-Al(1)-O(2)	90.36(10)	89.93(8)
O(1)-Al(1)-O(3)	89.29(11)	88.65(7)
O(1)-Al(1)-O(4)	84.02(7)	83.80(8)
O(2)-Al(1)-O(2)'	97.39(16)	98.66(11)
O(2)-Al(1)-O(3)	85.93(12)	85.53(8)
O(2)-Al(1)-O(4)	99.85(10)	100.86(6)
O(1)-Al(4)-O(1)'	88.21(8)	88.30(6)
O(1)-Al(4)-O(1)"	91.79(8)	91.70(6)
	Tetrahedral coordination	
O(1)-Al(2)-O(1)'	110.60(6)	110.92(5)
O(1)-Al(2)-O(3)	108.32(7)	107.99(5)
O(2)-Al(3)-O(2)'	105.81(9)	105.14(6)
O(2)-Al(3)-O(5)	115.3(13)	113.51(5)
O(2)-Al(5)-O(2)'	101.5(13)	
O(2)-Al(5)-O(4)	104.2(9)	
O(2)-Al(5)-O(6)	116.3(15)	
O(4)-Al(5)-O(6)	112.7(27)	

4b. The two layers correspond to the compositional difference; the outer part contains no K^+ and the inner no NH_4^+. This type of diffusion is very different from the normal compositional profile of NH4-K during ion exchange (Fig. 4a). The progress of the exchange front in the case of NH4-K during NH_4^+ ion exchange is shown in Fig. 5. The progress of the exchange front becomes extremely sluggish as exchange proceeds, especially beyond 50–60 μm.

2. Composition and Structure

The chemical compositions of NH4-K, and NH4-B are listed in Table I. The starting $Na_{1.2}$ β-alumina was determined to be $Na_{1.2}Al_{11.0}O_{17.1}$, and chemical analysis of the resulting NH4-K revealed NH_3 = 3.41 ±

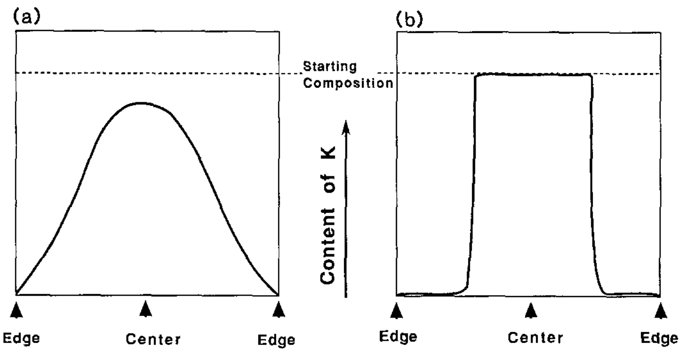

FIG. 4. The profile of potassium content in the *c*-plane across single crystals during NH_4^+ ion exchange for (a) NH4-K and (b) NH4-B.

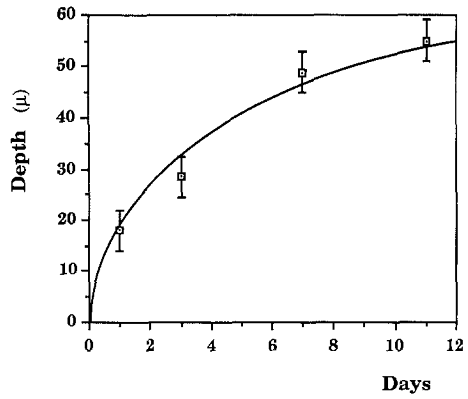

FIG. 5. The progress of ion-exchange front during NH_4^+ ion exchange for NH4-B.

0.02 wt%, and Na = 0.032 ± 0.006 wt%. Ignition loss was about 5.20 wt%. The amount of NH_3 clearly indicated the existence of excess NH_4^+ ions in the structure. These values were consistent with the calculated ones (total ignition loss = 5.27 wt%, and NH_3 = 3.45 wt%) for the expected formula $(NH_4^+)_{1.2}Al_{11}O_{17.1}$. Structure refinement also proved the existence of excess NH_4^+ ions in the conduction plane and clearly showed the Frenkel defect of the Al^{3+} ion in the spinel block which takes place in the case of nonstoichiometric composition. (For the defect mechanism allowing nonstoichiometry in β-alumina, see Ref. (*30*).) The present result agrees with the works of Colomban *et al.* (*6*) and Newsam *et al.* (*8*) essentially. On the basis of the data of NH_3 analysis and ignition loss, no H_3O^+ species can be assumed to exist, which agrees with the works (*4, 15*) using the IR method. This result indicates that the nonstoichiometry was maintained through the ion-exchange reaction. The lattice parameters measured on several single crystals were in the ranges a = 5.597–5.598 Å and c = 22.867–22.876 Å on the four-circle X-ray diffractometer. These values are also well consistent with the previous papers (*2, 8*). In conclusion, β-alumina containing 20–30% excess cations (Na^+ and K^+) was converted into NH_4^+ β-alumina maintaining the nonstoichiometry (defects) under the previously described conditions.

In the case of NH4-B, the content of NH_3 was 3.1 ± 0.1 wt% and total ignition loss was 4.4 wt%. (The content of the remaining Ba^{2+} and K^+ was a negligible amount.) Structure refinement revealed the existence of just a stoichiometric amount of NH_4^+ ion at the BR site and no apparent defects. These facts indicate a stoichiometric composition, $(NH_4)_{1.0}Al_{11.0}O_{17.0}$, for NH4-B. The calculated NH_3 content is 2.90 wt% and total ignition loss is 4.43 wt% for the ideal $(NH_4)_{1.0}Al_{11.0}O_{17.0}$. The lattice parameters measured on several single crystals were in the ranges a = 5.5984–5.5988 Å and c = 22.843–22.848 Å on the four-circle X-ray diffractometer. If the nonstoichiometry were retained, the expected product would be $(NH_4)_{1.5}Al_{11.0}O_{17.25}$, for which calculated values were 4.26 wt% for NH_3 content and 6.25 wt% for total ignition loss. However, the characterization result clearly showed that the excess cations were removed, and that the compound has changed into stoichiometric β-alumina during the NH_4^+ ion-exchange reaction. As described before, a similar phenomenon was reported in NH_4^+ β-gallate (*16, 17*). However, this is the first time that in the β-alumina system such an elimination of excess cations during NH_4^+ ion exchange takes place. So, the number of excess cations can not always be assumed to be retained through NH_4^+ ion exchange even in the β-alumina system.

The differences of the exchange reaction of two different K β-aluminas may be caused by the factors such as (i) the amount of excess cations in the starting β-alumina ($x = 0.2$ for NH4-K, and $x = 0.5$ for NH4-B) and (ii) the size of the crystal (thickness in the basal plane: 500 μm for NH4-K, and 100 μm for NH4-B). The cause of the different exchange reactions is now under investigation. Preliminary study showed that the prolonged exchange (up to 6 weeks) of tiny $K_{1.2}$ β-alumina crystals (about 100 μm in the *c*-plane) lead to the decrease of the *c*-axis parameter (to 22.84 Å). The different behavior may be attributed to the size of the crystal. Further study is in progress (*31*).

Another point to be noticed is that the *c*-axis parameter of the obtained stoichiometric NH_4^+ β-alumina is only a little smaller than that of the nonstoichiometric one (Table I). So far, it was assumed that the large decrease in the *c*-axis would occur if there is no *mO* site occupation of NH_4^+, and the discussion of the structure was based on this assumption (*8*). However, this assumption proved not to be valid.

In relation to the *c*-parameter, it was pointed out (*28*) that the *c*-parameter does not necessarily increase according to the reduction of population on the conduction plane as generally believed. The *c*-parameter is composed of the mirror plane thickness (M_{12k}) and the spinel block thickness (S_{12k}) (the equation is $c = 2\ (M_{12k} + S_{12k})$, and M_{12k} is the distance between O(2) across the mirror plane), and we found that M_{12k}, not the *c*-parameter, generally increases according to the reduction of population on the conduction plane. See Ref. (*32*) for details. In the present case, M_{12k} for NH4-K (nonstoichiometric) is 4.837 Å and that for NH4-B (stoichiometric) is 4.850 Å though the *c*-parameter of NH4-B is smaller, so it also follows the general rule we have proposed.

The data of lattice parameters offer a clue to interpret the thermal behavior of NH_4^+ β-alumina.

3. *Thermal Behavior*

TGA/DTA was carried out on NH4-K and NH4-B. In the case of NH4-K, the weight loss can be divided into three stages (Fig. 6): (1) 0.79 wt% at 170–350°C (2) 2.80 wt% at 350–600°C (3) 1.48 wt% at 750–1000°C. Stages 1 and 2 are continuous and may be overlapped, but are discerned by the change of slope. In air, DTA event was observed at 280°C (minor), 380°C, 790°C, and 1060°C, which are all exothermic reactions. Exothermic behavior did not change in a dry nitrogen atmosphere. The first exothermic event takes place in stage 1, and the second starts at the beginning of stage 2. In the case of NH4-B, the weight loss consists of only two stages (Fig. 7): (1) 2.82 wt% at 300–550°C (2) 1.44 wt% at 740–1000°C. The exothermic peaks were observed at 365, and 770, and 1070°C.

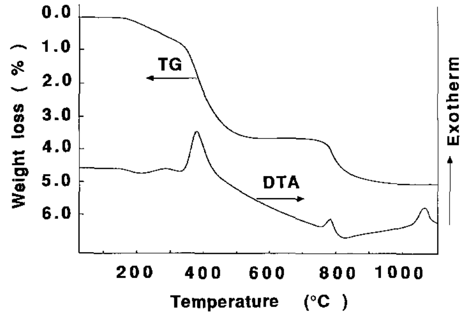

FIG. 6. Thermal analysis of NH4-K. The heating rate was 5°C/min.

The thermal decomposition of nonstoichiometric NH_4^+ β-alumina was already reported by several researchers. Newsam *et al.* (*8*) reported the similar decomposition schemes in the case of $(NH_4^+)_{1.3}$ β-alumina. They reported the three stages of thermal decomposition: (1) 0.83 wt% at 250–350°C

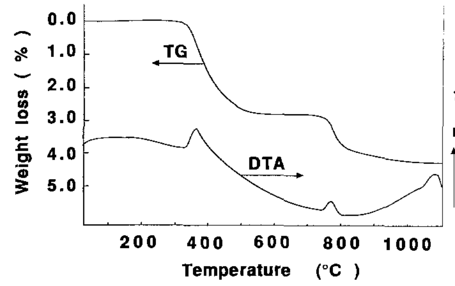

FIG. 7. Thermal analysis of NH4-B. The heating rate was 5°C/min.

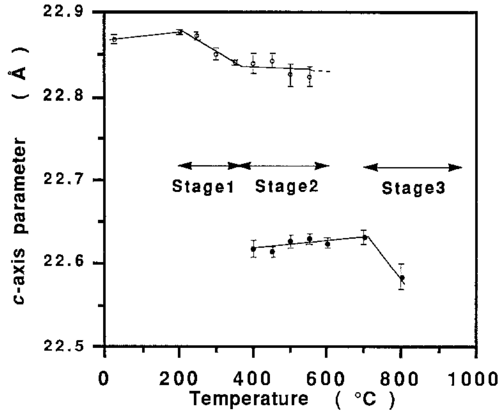

FIG. 8. The *c*-axis parameters plotted against temperature for NH4-K.

(2) 2.82 wt% at 350–580°C (3) 1.64 wt% at 580–1000°C. The accumulated weight loss was 5.29 wt%. These values are consistent with our result of NH4-K. Their interpretation of the decomposition process was as follows: At stage 1 $(NH_4^+)_{1.3}Al_{11}O_{17.15}$ releases excess NH_3. At 350°C, the composition was assumed to be $(NH_4)_{1.00}H_{0.25}Al_{11}O_{17.125}$. In stage 2, NH_3 is further released with leaving H^+ in the structure, the amount of interstitial ions is retained at first, but then interstitial ions decrease toward the end of stage 2. NH_4^+ ions were also assumed to be distributed among the *mO* site and the *BR* site, and rearrangement of NH_4^+ ions among these sites takes place at about 420°C, causing an exothermic event.

Their scheme was based on two assumptions: (i) the stoichiometric NH_4^+ β-alumina would have a much smaller *c*-axis parameter (near 22.66 Å) than the nonstoichiometric one, (ii) interstitial ions exist in stage 2 up to 570°C. The *c*-axis parameter at each stage was reported (*4*, *8*): 22.87 Å before stage 1, 22.86–22.84 Å at the beginning of stage 2 (ca. 350°C) and 22.66 Å at the end of stage 2 (ca. 580°C). As the observed *c*-parameter at stage 2 is larger than they supposed, they considered the continued occupation of the *mO* site even though a second ammonium site is not demanded. However, the assumption is contrary to the fact as pointed out before. The stoichiometric NH_4^+ β-alumina has the *c*-axis parameter of 22.84 Å, which is only a little smaller than that of the nonstoichiometric NH_4^+ β-alumina (22.87 Å). As for the amount of the interstitial Al and O at high temperature, supplemental experiments were made (*32*). NH4-K single crystals of 100–200 μm were heated up to 350, 370, and 390°C at the rate of 2°C/min, held for 0.5 hr, and cooled to room temperature. The resulting *c*-parameters were 22.856, 22.851, and 22.847 Å, respectively. The structural refinement of the 370°C treated single crystal ($R = 0.025$, $wR = 0.032$ $w = 1/\sigma F^2$) revealed a drastic decrease of the occupancy of *i*Al (0.1 per unit cell), and *i*O. The difference Fourier maps at $z = 0.18$ and 0.25 are shown in Figs 1b and 2b, which show clearly the rapid decrease of interstitial ions in stage 1. The interstitial ions cannot be assumed to exist in stage 2.

High temperature powder diffraction was conducted to see the change of the lattice parameters. In Fig. 8, the present result of *c*-axis length of NH4-K vs temperature is given. The stage of thermal behavior is indicated in the figure. Before stage 1, the *c*-axis length increases to 22.88 Å due to thermal expansion; in stage 1, the length decreases to 22.84 Å. Tofield *et al.* (*4*) stated that two *c*-axis lattice parameters, $c = 22.66$ Å and $c = 22.84$ Å, coexist between 400 and 600°C, and that the former became dominant at higher temperature at the expense of the latter. This phenomenon was confirmed by the present study. Two phases of β-alumina structure appear in stage 2 (350–600°C). At the end of this stage, $c = 22.84$ Å could not be detected. At stage 3, the *c*-axis parameter decreases rapidly and no β-alumina phase could be found beyond 900°C, indicating decomposition of fundamental β-alumina structure.

By comparing stoichiometric with nonstoichiometric NH_4^+ β-alumina, the thermal behavior can be interpreted more clearly. It seems that the first stage of NH4-K lacks in the case of NH4-B, and that stage 1 of NH4-B corresponds to stage 2 of NH4-K, though the starting temperature is slightly shifted down temperature (300°C) in the case of NH4-B. At the end of the first stage the c-axis parameter is 22.84 Å. Considering the 22.84 Å of the c-axis parameter in the case of stoichiometric NH_4^+ β-alumina (NH4-B), the first stage would be the conversion of NH4-K into stoichiometric NH_4^+ β-alumina. At the beginning of stage 2, an exothermic reaction takes place. The exothermic peak can not be attributed to the rearrangement of NH_4^+ ions among the ammonium sites, because a similar peak can be observed in $(NH_4)_{1.0}$ β-alumina in which NH_4^+ ions occupy only the *BR* site. This may be due to the conversion into $H^+Al_{11}O_{17}$ caused by the elimination of NH_3 from the *BR* site in the conduction plane, not to the rearrangement of NH_4^+ ions. A dramatic decline of the ionic conductivity was reported to take place beyond 350°C (7). This may be because there is less than one NH_4^+ ion at the BR site in one conduction plane beyond 350°C and because the conduction mechanism changes from an interstitial type to a vacancy type. The coexistence of two phases in stage 2 (350–600°C) may be because two β-aluminas, $(NH_4)_{1.0}Al_{11}O_{17}$ (c = 22.84 Å) and $HAl_{11}O_{17}$ (c = 22.66 Å), are immiscible with each other and form two compositional domains.

The thermal behavior of $(NH_4)_{1.2}$ β-alumina can be summarized as follows: It consists of three stages. (1) Stage 1 is at 200–350°C. Excess NH_4^+ ions are eliminated together with interstitial oxygen, leading to stoichiometric NH_4^+ β-alumina, $(NH_4)_{1.0}Al_{11}O_{17}$. In the stoichiometric NH_4^+ β-alumina, NH_4^+ ions occupy only the *BR* site. The c-axis parameter changes from 22.87 to 22.84 Å. (2) Stage 2 is at 350–600°C. NH_3 is eliminated from the conduction plane, leading to $HAl_{11}O_{17}$. Two immiscible β-alumina phases ($(NH_4)_{1.0}Al_{11}O_{17}$: c = 22.84 and $HAl_{11}O_{17}$: c = 22.66 Å) coexist in this temperature range, and $HAl_{11}O_{17}$ becomes dominant at higher temperature. (3) Stage 3 is at 700–1000°C and is the final decomposition to Al_2O_3. As for the DTA event, the exothermic peak at around 380°C is due to the transformation into $H^+Al_{11}O_{17}$ caused by the loss of ammonia from the BR site; the exothermic peak at 760°C is due to the conversion of β-alumina to a disordered spinel structure. From the above assumption, (1) 0.88 wt% for stage 1 (2) 2.57 wt% for stage 2 (3) 1.82 wt% for stage 3, and 5.27 wt% for the total loss is expected.

Acknowledgments

The authors are very grateful to Dr. S. Takekawa for providing us single crystals of Ba β-alumina, and to Drs. T. Mitsuhashi and Y. Matsui of our institute (NIRIM) for suggestions and technical help and to Dr. S. Hishita for suggestions on diffusion. Thanks are also due to Mr. K. Kosuda (NIRIM) for help in electron probe microanalysis.

References

1. VON H. SAALFELD, H. MATTHIES, AND S. K. DATTA, *Ber. Dtsch. Keram. Ges.* **45,** 212 (1968).
2. Y. F. Y. YAO AND J. T. KUMMER, *J. Inorg. Nucl. Chem.* **29,** 2453 (1967).
3. PH. COLOMBAN, J. P. BOILOT, P. CHAGNON, AND G. GUILLOTEAU, *Bull. Soc. Fr. Céram.* **119,** 3 (1978).
4. B. C. TOFIELD, J. M. NEWSAM, AND A. HOOPER, *Solid State Ionics* **5,** 249 (1981).
5. N. BAFFIER, J. C. BADOT, AND PH. COLOMBAN, *Solid State Ionics* **13,** 233 (1984).
6. PH. COLOMBAN, J. P. BOILOT, A. KAHN, AND G. LUCAZEAU, *Nouv. J. Chim.* **2,** 21 (1978).
7. A. HOOPER, B. C. TOFIELD, AND C. F. SAMPSON, *in* "Fast Ion Transport in Solids" (Vashishita, Mundy, and Shenoy, Eds.), p. 409, Elsevier North Holland, Amsterdam (1979).
8. J. M. NEWSAM, A. K. CHEETHAM, AND B. C. TOFIELD, *Solid State Ionics* **8,** 133 (1983).
9. J. D. AXE, L. M. CORLISS, AND J. M. HASTINGS, *J. Phys. Chem. Solids* **39,** 155 (1978).
10. J. C. LASSEGUES, M. FOUASSIER, N. BAFFIER, PH. COLOMBAN, AND A. J. DIANOUX, *J. Phys.* **41,** 273 (1980).
11. H. ARRIBART, H. CARLOS, AND B. SAPOVAL, *Solid State Ionics* **5,** 253 (1981).

12. J. O. Thomas, and G. C. Farrington, *Acta Crystallogr Sect. B* **39,** 227 (1983).
13. G. C. Farrington and J. L. Briant, *in* "Fast Ion Transport in Solids" (Vashishita, Mundy, Shenoy, Eds.), p. 395, Elsevier North Holland, Amsterdam (1979).
14. N. Iyi, A. Grzymek, and S. Nickolson, *Solid State Ionics* **37,** 11 (1989).
15. Ph. Colomban and A. Novak, *Solid State Ionics* **5,** 241 (1981).
16. H. Ikawa, T. Tsurumi, M. Ishimori, K. Urabe, and S. Udagawa, *J. Solid State Chem.* **60,** 51 (1985).
17. H. Ikawa, T. Tsurumi, K. Urabe, and S. Udagawa, *Solid State Ionics* **20,** 1 (1986).
18. B. C. Tofield, A. J. Jacobson, W. A. England, P. J. Clarke, and M. W. Thomas, *J. Solid State Chem.* **30,** 1 (1979).
19. S. Takekawa, *in* "Research Report of NIRIM, 37", 15, NIRIM (1983).
20. N. Iyi, S. Takekawa, and S. Kimura, *J. Solid State Chem.* **59,** 250 (1985).
21. N. Iyi, Z. Inoue, and S. Kimura, *J. Solid State Chem.* **61,** 81 (1986).
22. W. R. Busing and H. A. Levy, *Acta Crystallogr.* **10,** 180 (1957).
23. J. A. Ibers and W. C. Hamilton, "International Tables for X-ray Crystallography," Vol 4, Kynich Press, Birmingham (1974).
24. T. Sakurai, K. Nakatsu, H. Iwasaki, and M. Fukuhara, RSFLS-4, UNICS II, The Crystallographic Society of Japan (1967).
25. T. Sakurai, RSSFR-5, UNICS II. The Crystallographic Society of Japan (1967).
26. P. J. Becker and P. Coppens, *Acta Crystallogr. Sect. A* **30,** 148 (1974).
27. C. R. Peters, M. Bettman, J. W. Moore, and M. D. Glick, *Acta Crystallogr. Sect. B* **27,** 1826 (1971).
28. N. Iyi, S. Takekawa, and S. Kimura, *J. Solid State Chem.* **83,** 8 (1989).
29. B. C. Tofield, *Solid State Ionics* **5,** 245 (1981).
30. W. L. Roth, F. Reidinger, and S. LaPlaca, *in* "Superionic Conductors" (G. D. Mahan and W. L. Roth, Eds.), p. 223, Plenum, New York (1977).
31. N. Iyi, Y. Yajima, and S. Kimura, submitted for publication.
32. N. Iyi, unpublished data.